ASPS Conference Proceedings 1: 625-630 (2022)

Proceedings of

12th Structural Engineering Convention - An International Event (SEC 2022)

Available at https://asps-journals.com/index.php/acp

Effect of Vertical Setbacks of Space Frame Structure under Seismic and Blast Loads using Applied Element Method

K. Hemanth Kumar [1, *], R.K. Tripathi [2]

[1] Department of Civil Engineering, Research Scholar, National Institute of Technology, Raipur, 492010, India
[2] Department of Civil Engineering, Professor, National Institute of Technology, Raipur, 492010, India

Paper ID - 060096

Abstract

Structures, when subjected to nonlinear dynamic loading, drastically affect the structure's physical properties. The structural failure occurred at the critical points of weakness during the earthquake. These structural weaknesses observed in irregular structures are mainly due to the improper distribution of mass, geometry and stiffness. Architects usually prefer irregular buildings for the aesthetics point of view. These irregular structures are more vulnerable to dynamic loading. On the other hand, the devastating failure due to bomb blast is also the concern for the study as many vital structures collapsed because of the terrorist attack. Such failures need to be checked by studying the performance of building under the earthquake and blast loading. The objectives of this paper are to compare the peak responses at each storey level of mass irregular space frame structure to the dynamic effect. Firstly, Time History of the Northridge earthquake spectra with Peak Ground Acceleration (P.G.A.) =8.660 m/s^2 = 0.883g at 9.82 seconds considered and analysed. Secondly, blast material [1] composed of two different charge weights [2] 1000 kg TNT and 2500 kg TNT at a distance of 10m was considered. For responses to the structure, the most advanced numerical tool viz., Applied Element Method (AEM) has been used. It is concluded that the amplitude of Northridge earthquake's maximum x-displacement at the terrace level is closer to maximum x-displacement for the blast load of 2500kg TNT but the time of occurrence was changed abruptly, i.e., Northridge earthquake maximum displacement occurs at the duration of nearly 10 sec, but the maximum displacement of blast load of 2500kg TNT is occurring almost at 0.2 sec, i.e., 50 times quicker in occurrence.

Keywords: Applied Element Method, X-displacement, X- Acceleration, Northridge Earthquake, Blast loads of 1000kg TNT & 2500kg TNT

1. Introduction

Studies of structure collapse for high magnitude earthquakes and large blast charges kept by terrorists are very vital to reduce the deaths. Initially, the small structure displacements can be observed, followed by large displacements at each level before the collapse. In the small displacement range, structure geometry changes can be neglected during loading. The primary reason for structural failure is because of buckling of columns can only be detected by the theory of large displacement.

The popular numerical tool, i.e. Finite Element Method (FEM) has been considered for studying the behaviour of structural buckling. By using this tool, the buckling mode for the load, and also the behaviour of post-buckling can be followed. Unfortunately, the FEM has problems in material separation because of the assumption that material is a continuum and innovative tools must be adopted to consider the separation of structural members.

Modified or Extended Distinct Element Method (EDEM) [7] [8] is the tool that deals with structure failure analysis. Primary disadvantage of this method is that it is less accurate in the small displacement range. It requires relatively more CPU time when compared to the FEM. The Rigid Body and Spring Model (RBSM) [4] [5] methodology adopt rigid elements, but not checked for buckling analysis. The concepts of RBSM, EDEM and FEM. [6] used in the evolution of the most potent tool, i.e., Applied Element Method (AEM) [9]

2. Applied Element Method Overview

Unlike FEM, the elements in AEM are connected by normal and shear springs distributed over each element contact surface. Figure 1 shows the division of a structure into elements and the connection of elements through springs. The stiffness of each pair of normal and shear springs connecting the element centrelines is calculated as in Equations (1) and (2).

$$k_s = \frac{G \times d \times t}{a} \quad (1)$$

$$k_n = \frac{E \times d \times t}{a} \quad (2)$$

Where, E & G are Elastic Modulus and Modulus of Rigidity, respectively, 'd' is the springs spacing, 't' is the element thickness, and 'a' is the representative area's length.

*Corresponding author. Tel: +919491772645; E-mail address: khkumar.phd2019.ce@nitrr.ac.in

Published online: December 19, 2022
doi:10.38208/acp.v1.562

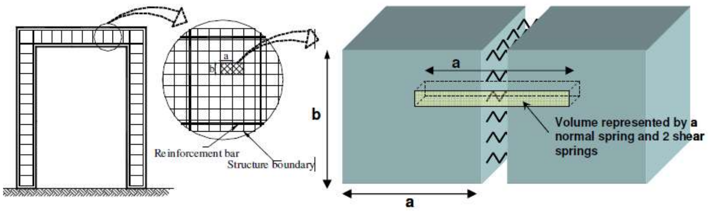

Fig. 2(a). AEM structural modelling [3] [9]

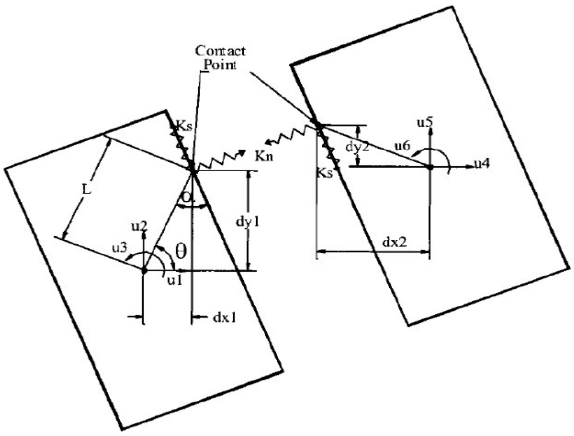

Fig. 2(b). Element shape, contact point and DOF [11]

In the 2D model, each element has 3 DOF. The size of element stiffness matrix is 6 x 6. The element stiffness matrix is determined by equation 5 [11]

The governing equation for large deformation dynamic analysis is [11]

$$[M]\Delta\ddot{u} + [C]\Delta\dot{u} + [K]\Delta u = \Delta f(t) + R_M + R_G \qquad (4)$$

Where,

$\Delta\ddot{u}$ is acceleration, $\Delta\acute{u}$ is velocity, Δu is displacement,

R_G is Geometrical residual forces, R_M is the residual load vector due to cracking or incompatibility between spring stress and the corresponding strain (Meguro and Tagel- Din, 2002), Mass matrix [M], Damping Matrix [C] and Incremental applied load vector $\Delta f(t)$.

Matrix of global nonlinear stiffness [K]:-

$$[K] = \begin{bmatrix} sin^2(\theta+\alpha)k_n + cos^2(\theta+\alpha)k_s & -k_n sin(\theta+\alpha)cos(\theta+\alpha) + k_s sin(\theta+\alpha)cos(\theta+\alpha) & cos(+\alpha)k_s c\ sin(\alpha) - sin(\theta+\alpha)k_n L cos(\alpha) \\ -k_n sin(\theta+\alpha)cos(\theta+\alpha) + k_s sin(\theta+\alpha)cos(\theta+\alpha) & sin^2(\theta+\alpha)k_s + cos^2(\theta+\alpha)k_n & cos(\theta+\alpha)k_n L cos(\alpha) + sin(\theta+\alpha)k_s L sin(\alpha) \\ cos(\theta+\alpha)k_s L\ sin(\alpha) - sin(\theta+\alpha)k_n L cos(\alpha) & cos(\theta+\alpha)k_n L cos(\alpha) + sin(\theta+\alpha)k_s L sin(\alpha) & L^2cos^2(\alpha)k_n + L^2 sin^2(\alpha)k_s \end{bmatrix}$$

(5)

Where, L is the distance between the spring location and the element centroid, and θ and α are the element orientation angles [11] [13].

3. Irregular building description

3.1 Sectional and reinforcement details

A (G+4) storey Irregular Space Frame as shown in Fig. 3(a) was used as a case study. The structure we considered was initially designed using design software, i.e., STAAD Pro., for all combinations of loads according to IS-456:2000 & IS-875(part 5) code provisions. Later the analysis of that structure was analysed by an efficient tool, Applied Element Method (AEM). In this study for AEM model, the element size and number of springs are fixed for accurate results. The dimensions of the frame, reinforcement details, and loadings are shown in figures. The material properties used for the analysis of structure are tabulated below in Fig 3(a).

Material properties	Concrete	Steel
Modulus of elasticity, MPa	25000	200000
Compressive strength, MPa	25	-
Modulus of Rigidity, MPa	9060	76940
Tensile strength, MPa	3.0	550
Separation strain	0.20	0.20
Coefficient of Friction	0.8	0.8
Ultimate strain	-	0.1

Fig. 3(a). Properties of materials

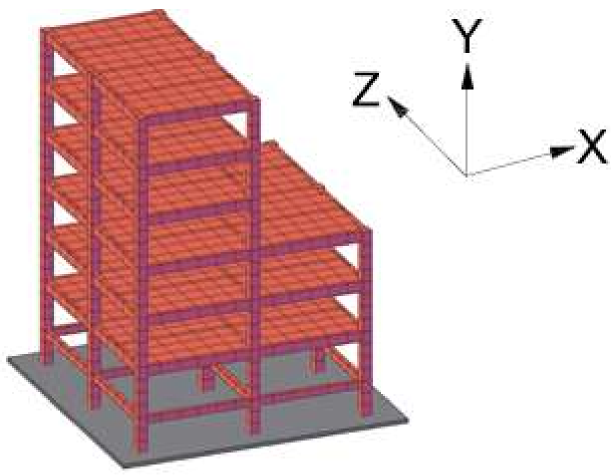

Fig. 3(b). 3-D model with elements

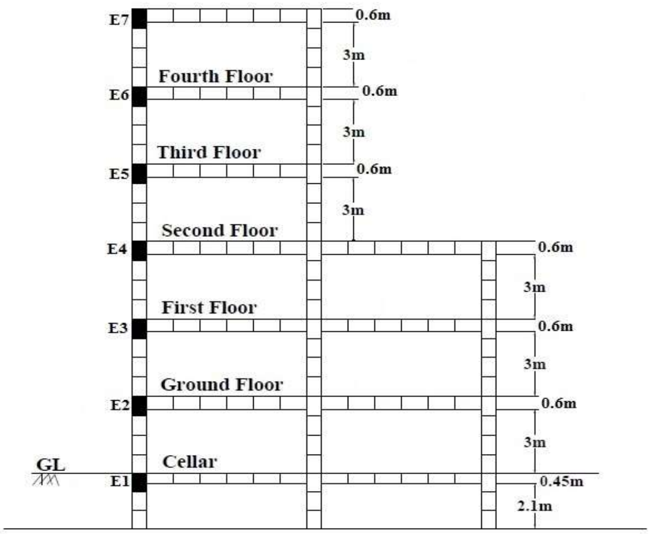

Fig. 3(c). Elevation of model

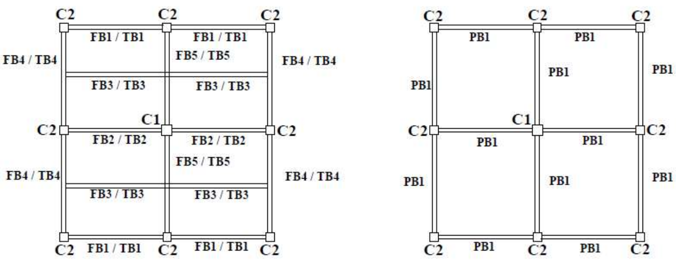

Fig. 3(d) Beams and Columns detail sectional plan

3.2 Concrete sectional details

Plinth beam PB1 of size 0.3m x 0.45m.
Floor beams FB1, FB2, FB3, FB4 & FB5 are of size 0.3m x 0.6m each.
Terrace beams TB1, TB2, TB3, TB4, TB5 are of size 0.3m x 0.6m each.
Columns C1 & C2 are of size
0.75m x0.75m & 0.6mx0.6m respectively.
Considering the thickness of the slab as 150 mm

3.3 Reinforcement details

Slab

Shorter span – 8 dia @ 150mm c/c
Longer span – 8 dia @ 200mm c/c

Columns

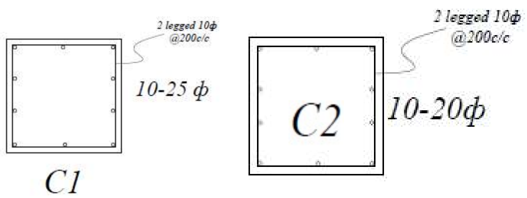

Fig. 3(e). Columns sectional reinforcement details

Beams

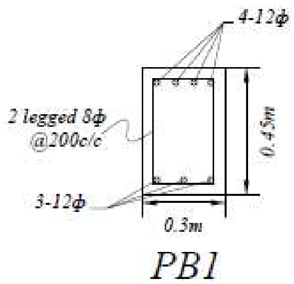

Fig. 3(f). Plinth beam sectional reinforcement details

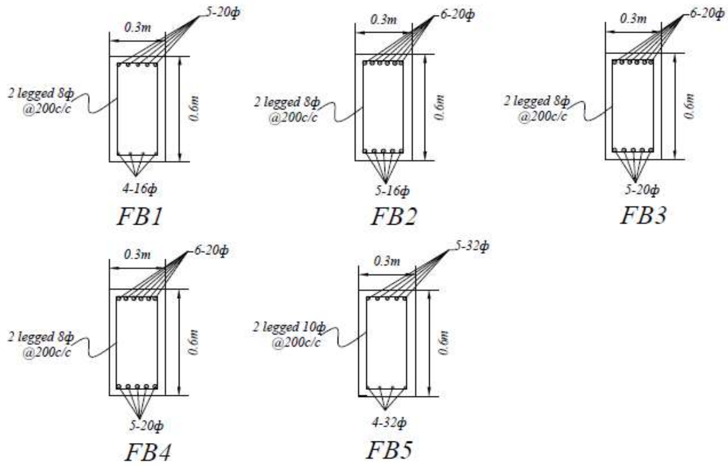

Fig. 3(g). Ground, 1st, 2nd, 3rd & 4th floor beams sectional reinforcement details

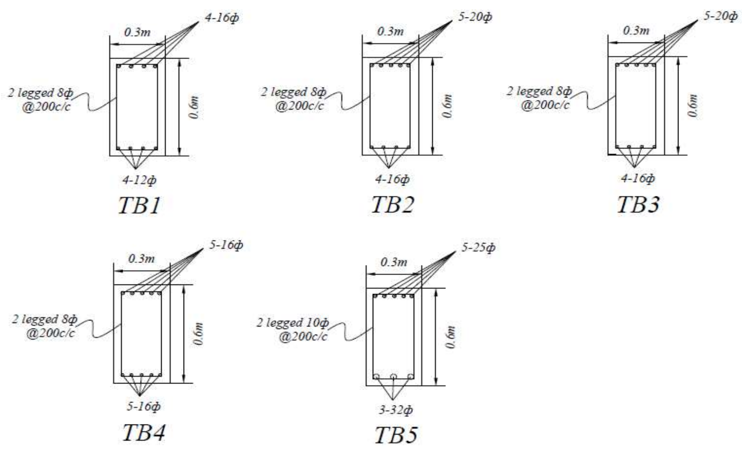

Fig. 3(h). Terrace beams sectional reinforcement details

4. Dynamic Loading Conditions

The following are the case studies used for the analysis

Case i:

The self-weight of the frame, in addition to this Northridge earthquake (Santa Monica City Hall Grounds Channel 1, 90 Degrees, 04:31 PST, January 17, 1994) spectra [10] shown

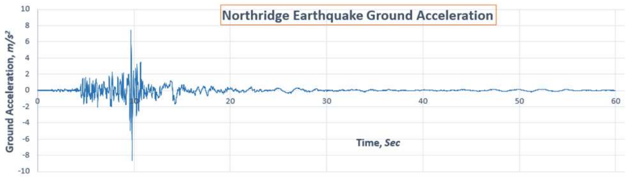

Fig. 4(a). Northridge Earthquake ground motion

in Fig. 4(a) with Peak Ground Acceleration *P.G.A., =8.660 m/s2 = 0.883g at 9.82 seconds,* was considered and analysed using AEM. Time effects since the start of loading [12] until the end of the analysis are continuous. For the structure non-linear dynamic analysis, a numerical solution from dynamic equation to obtain X-displacements for each stage was adopted.

Case ii:

The blast material composed of charge weight 1000kg TNT at a distance of *R*=10m from the side face offset to the central column of the building was considered. For the present case on the non-linear dynamic X-displacement of defined structure elements (shown in Fig. 5(b).) subjected to blast load was considered.

Case iii:

The blast material composed of charge weight 2500kg TNT at a distance of *R*=10m from the side face offset to the central column of the building was considered. For the present case on the non-linear dynamic X-displacement of defined structure elements (shown in Fig. 5(c).) subjected to blast load was considered.

5. Results & Discussion

Case i: Northridge earthquake is applied

For the non-linear dynamic analysis, the earthquake load considered for the simulation is Northridge ground motion. The responses observed in the simulation of (G+4) storey irregular frame by AEM, the elements defined in Fig. 3(c) for each level of front face corner end, the X- Displacement values gradually increasing, i.e., max +ve 5.60 mm at 11.8 sec and min –ve 6.41 mm at 10.2 sec, max +ve 24.32 mm at 11.8 sec and min –ve 24.86 mm at 10.2 sec, max +ve 42.64 mm at 11.8 sec and min –ve 41.36 mm at 10.2 sec, max +ve 58.98 mm at 11.8 sec and min –ve 57.5 mm at 11 sec, max +ve 74.58 mm at 10.2 sec and min –ve 73.44 mm at 10.44 sec, max +ve 88.25 mm at 10.2 sec and min –ve 84.87 mm at 5 sec, max +ve 98.18 mm at 10.2 sec and min –ve 95.75 mm at 10.8 sec for E1, E2, E3, E4, E5, E6, E7 respectively.

Storey Level	**Time vs X-Displacement**
(Plinth) +0m level	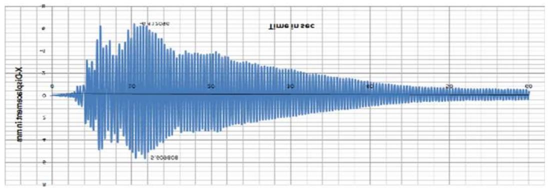
+3m level	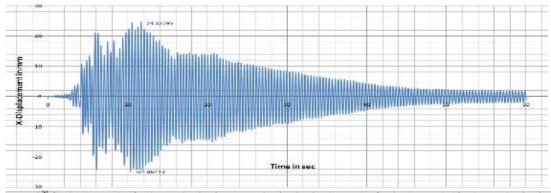
+6m level	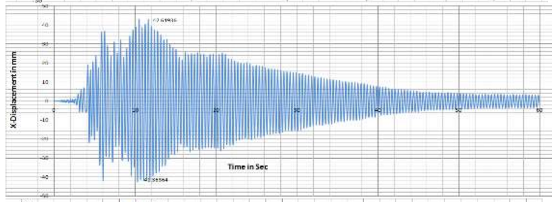
+9m level	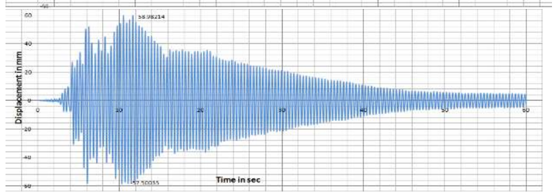
+12m level	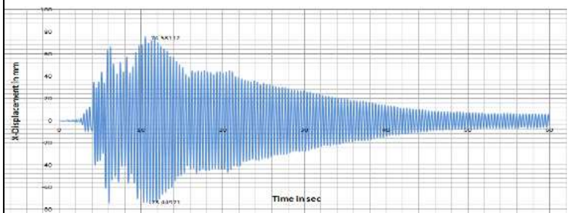
+15m level	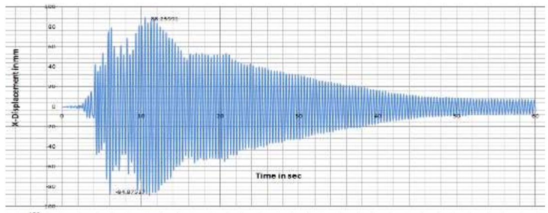
(Terrace) +18m level	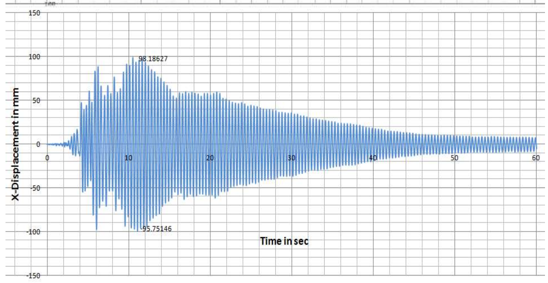

Fig. 5(a). X-displacement for Northridge earthquake

Case ii: Blast Load of 1000kg TNT is applied

In case II, the X- Displacement values gradually increasing i.e., max +ve 3.5 mm at 0.6 sec and min –ve 4.2 mm at 0.3 sec, max +ve 14.41 mm at 0.62sec and min –ve 15 mm at 0.3

sec, max +ve 22.77 mm at 0.5sec and min –ve 21.87 mm at 0.7 sec, max +ve 27.36 mm at 0.6 sec and min –ve 26.44 mm at 0.8 sec, max +ve 29.45 mm at 0.2 sec and min –ve 31.43 mm at 0.8 sec, max +ve 41.28 mm at 0.2 sec and min –ve 36.59 mm at 0.4 sec, max +ve 51 mm at 0.18 sec and min –ve 48.42 mm at 0.4 sec for plinth (+0m), +3m, +6m, +9m, +12m, +15m, +18m levels respectively.

Storey Level	**Time vs X-Displacement**
(Plinth) +0m level	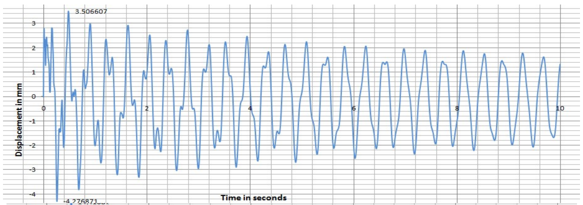
+3m level	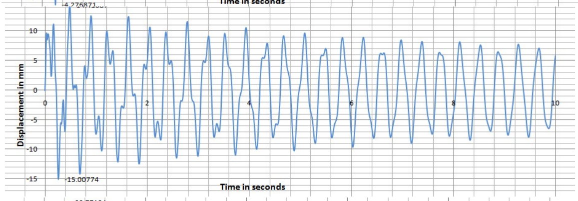
+6m level	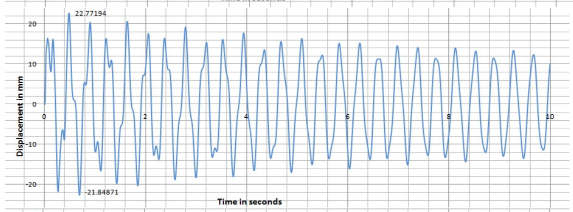
+9m level	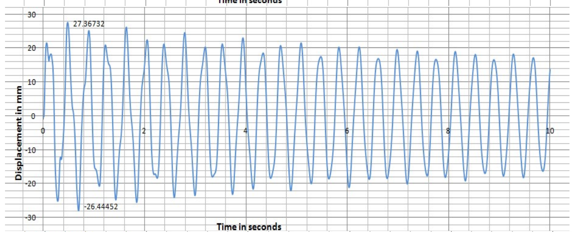
+12m level	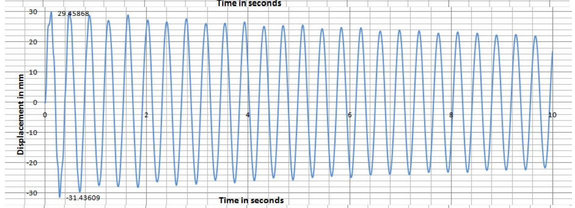
+15m level	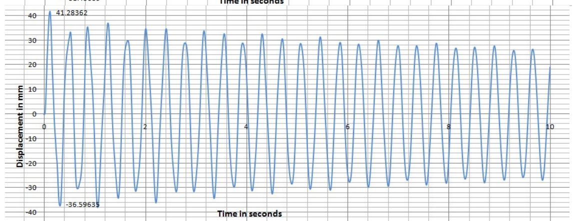
(Terrace) +18m level	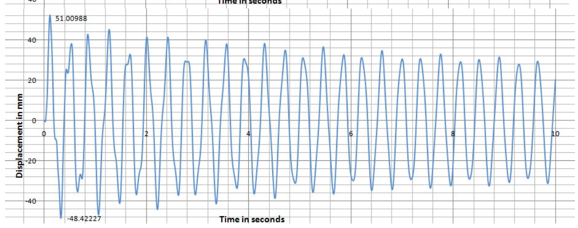

Fig. 5(b). X-displacement for 1000kg TNT

Case iii: Blast Load of 2500kg TNT is applied

In case III, the X- Displacement values gradually increasing i.e., max +ve 6.2 mm at 0.5 sec and min –ve 9.41 mm at 0.3 sec, max +ve 25.87 mm at 0.6 sec and min –ve 25.42 mm at

Storey Level	**Time vs X-Displacement**
(Plinth) +0m level	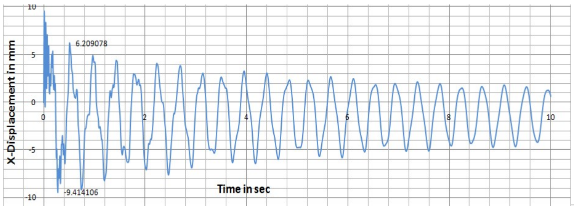
+3m level	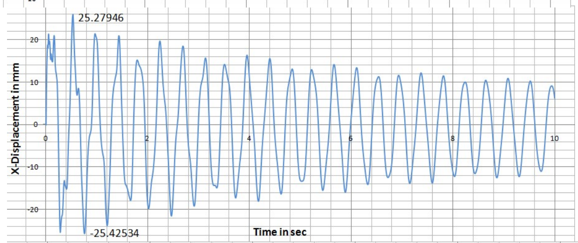
+6m level	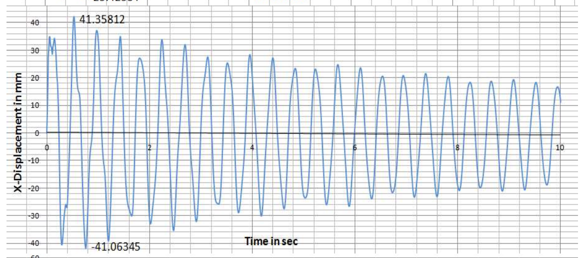
+9m level	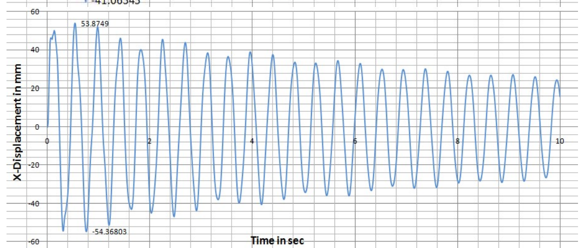
+12m level	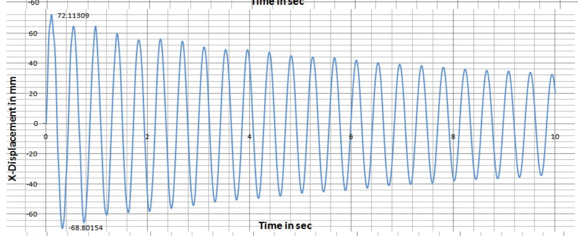
+15m level	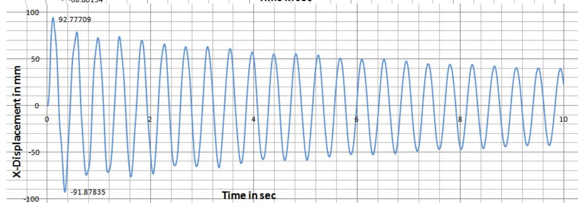
(Terrace) +18m level	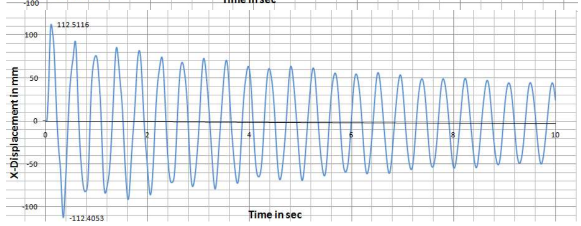

Fig. 5(c). X-displacement for 2500kg TNT

0.8 sec, max +ve 41.35 mm at 0.6 sec and min –ve 41.06 mm at 0.9 sec, max +ve 53.87 mm at 0.5 sec and min –ve 54.36 mm at 0.8 sec, max +ve 72.11 mm at 0.1 sec and min –ve 68.8 mm at 0.3 sec, max +ve 92.77 mm at 0.25 sec and min –ve 91.87m at 0.38 sec, max +ve 112.5 mm at 0.2 sec and min –ve 112.4 mm at 0.38 sec for plinth (+0m), +3m, +6m, +9m, +12m, +15m, +18m levels respectively.
From the results, it was observed that X-Displacement for each level, i.e., from plinth to the terrace of the structure increased abnormally within no time. In contrast, for blast loads increase and decrease periodically because of uneven moments acting on the structure for the impact of blast load onto the edge elements of the side face. The percentage increase in x-displacements for blast loads of 1000kg TNT when compared with 2500kg TNT are max +ve 43.54% and min –ve 55.36%, max +ve 44.29% and min –ve 40.99%, max +ve 44.93% and min –ve 46.80%, max +ve 45.33% and min –ve 42.54%, max +ve 42.75% and min –ve 46.81%, max +ve 55.50% and min –ve 60.17%, max +ve 54.41% and min –ve 56.92% for plinth (+0m), +3m, +6m, +9m, +12m, +15m, +18m levels respectively.

6. Conclusions

For Northridge earthquake, the x- displacement values vary from max +ve 5.60 mm at 11.8 sec and min –ve 6.41 mm at 10.2 sec to max +ve 98.18 mm at 10.2 sec and min –ve 95.75 mm at 10.8 sec, i.e., from plinth level to terrace level, increased gradually. For blast load of 1000kg TNT, the x-displacement values vary from max +ve 3.5 mm at 0.6 sec and min –ve 4.2 mm at 0.3 sec to max +ve 51 mm at 0.18 sec and min –ve 48.42 mm at 0.4 sec, i.e., from plinth level to terrace level, increased gradually. For blast load of 2500kg T.N.T., the x- displacement values vary from max +ve 6.2 mm at 0.5 sec and min –ve 9.41 mm at 0.3 sec to max +ve 112.5 mm at 0.2 sec and min –ve 112.4 mm at 0.38 sec, i.e., from plinth level to terrace level, increased gradually. The X- displacement for blast loads decreases harmonically with the increase in time. Northridge earthquake maximum x-displacement of the structure is nearer to maximum x-displacement for the blast load of 2500kg TNT but the time of occurrence was changed abruptly, i.e., Northridge earthquake maximum displacement occurs at the duration of nearly 10 sec, but the max displacement of blast load of 2500kg TNT is occurring almost at 0.2 sec i.e., 50 times quicker in occurrence. The percentage increase in x-displacements for blast loads of 1000kg TNT when compared with 2500kg TNT is ranging from 40% to 60% for a range of plinth level +0 to +18m level. The x-displacement of the earthquake shown similar variations for all storeys but the amplitude increases from plinth level to terrace level.

Disclosures

Free Access to this article is sponsored by SARL ALPHA CRISTO INDUSTRIAL.

References

1. A. Khadid et al. (2007), “ Blast loaded stiffened plates” Journal of Engineering and Applied Sciences, Vol. 2(2) pp. 456-461.
2. A. K. Pandey et al. (2006) “Non-linear response of reinforced concrete containment structure under blast loading” Nuclear Engineering and design 236. pp. 993-1002.
3. American Society for Civil Engineers 7-02 (1997), “Combination of Loads”, pp 239-244.
4. Kawai T., 1980. Some considerations on the finite element method, Int. J. for Numerical Methods in Engineering, 16, 81-120.
5. Kikuchi A., Kawai T., Suzuki N., 1992. The rigid bodies-spring models and their applications to three-dimensional crack problems, Comp. and Struct., 44(1), 469-480.
6. Kleiber M., 1989. Incremental finite element modeling in non-linear solid 33 Fig. 13 Load displacement relationship for a sway frame with hinged supports subjected to vertical loads mechanics, Ellis Horwood, New York
7. Meguro K. and Hakuno M., 1989. Fracture analyses of structures by the modified distinct element method, Struct. Engrg./Earthquake Engrg., 6(2), 283s-294s.
8. Meguro K. and Hakuno M., 1994. Application of the extended distinct element method for collapse simulation of a double-deck bridge, Struct. Engrg./Earthquake Engrg., 10(4), 175s-185s.
9. Tagel-Din, H. and Meguro, K., 1999. Applied element simulation for collapse analysis of structures, Bull. of Earthquake Resistant Struct. Res. Ctr., University of Tokyo, 32, 113-123.
10. Tagel-Din, H. and Meguro, K., 2000. Analysis of a small scale R.C. building subjected to shaking table tests using the applied element method, Proc. of 12th World Conf. on Earthquake Engrg., Auckland, New Zealand. Timoshenko S.
11. Tagel-Din, H. and Meguro, K. (2000). Applied Element Method for Dynamic Large Deformation Analysis of Structures. Structural Engineering / Earthquake Engineering JSCE, 17 (2), 9 pp.
12. Meguro, K. and Tagel-Din. H. (2001). Applied Element Simulation of RC Structures under Cyclic Loading. Journal of Structural Engineering ASCE, 127 (11), pp. 1295-1305.
13. Meguro, K. and Tagel-Din, H. S. (2002). Applied Element Method Used for Large Displacement Structural Analysis. Journal of Natural Disaster Science, 24 (1), pp. 25-34.